

Displacement-Based Formulation with Non-Penetration Constraint for Planar Composite Beams in Partial Interaction Using the Coupled Connector Model

Thaileng Oeng^{1,2*}, Pisey Keo³, Khandaker M. Anwar Hossain², Virak Han¹

¹ Faculty of Civil Engineering, Institute of Technology of Cambodia, Russian Federation Blvd., P.O. Box 86, Phnom Penh, Cambodia

² Department of Civil Engineering, Toronto Metropolitan University, Toronto, Canada

³ LGCGM/Structural Engineering Research Group, Univ Rennes - INSA de Rennes, Rennes, France

Received: 01 May 2024; Revised: 20 May 2024 Accepted: 01 June 2024; Available online: December 2024

Abstract: This research paper presents a finite element approach for the analysis of composite (two-layer) beams, with a steel bottom layer and a concrete top layer. These layers function as a planar composite beam interconnected by connectors. Issues arise at the interfaces of different materials (steel and concrete), leading to slip and uplift. The connector element consists of two-directional coupled springs: a horizontal spring parallel to the contact surface captures slip, while a vertical spring orthogonal to the contact surface captures uplift. The vertical spring activates only if there is separation between the layers; otherwise, contact forces exist. The analysis employs a geometrically nonlinear finite element formulation for planar composite structures, considering non-penetration conditions. The co-rotational method decomposes the element's motion into rigid body motion and small deformations. When material behavior becomes nonlinear, the finite element method based on the displacement-based formulation is commonly used. To prevent penetration between the layers, contact resolution methods such as augmented Lagrangian methods with Uzawa updating schemes are employed. Finite element models are used to conduct a parametric study to investigate the performance of the displacement-based formulation and the influence of using the interaction effect of shear and tensile behavior of the connector (coupled connector model) with the non-penetration condition. The performance of the proposed formulation is assessed through numerous numerical applications.

Keywords: Co-rotational, Displacement-based formulation, Non-penetration, Augmented Lagrangian method, Interlayer slip and uplift

1. INTRODUCTION

Over nearly a century, structural composite members consisting of semi-rigidly connected layers have been used by engineers. The overall behavior of such members strongly depends on the stress transfer mechanism between each layer which may be accomplished by either bond or shear connectors. The aspects of force transmission in composite member have been studied analytically and numerically by a great deal of research. The first contribution in the study of composite beams in partial interaction is commonly attributed to [1] who investigated the behavior of a two-layer beam considering that both layers are elastic and deform according to the Eurler-Bernoulli kinematics. In their paper, a closed-form solution is provided for a simply supported elastic composite beams. Since then, numerous analytical models were developed to study and model different aspects of the behavior of two-layer composite beams in more complicated

situations. To investigate the behavior of elastic two-layer beam, several analytical formulations were proposed [2-7]. Most of the papers on composite beams are focused on the effects of interlayer slip while uplift effects have been neglected. Only a small number of mathematical models take into account both slip and uplift at the interface. The first attempt is contributed by [8] who considered linear elastic behavior of simply supported composite beam. They constructed the governing equation of the system and solved it by using finite difference method. Later, [9] developed discrete shear connection model to perform an ultimate state analysis of composite beam by taking into account the effects of uplift at the steel-concrete interface. The vertical separation (positive uplift) and the compressibility (negative uplift) of one layer bearing on the other was considered in [9] by imposing the inequality constraint. Then, [10] have tackled the uplift problem at the interface of two-layer beam in a different way. They integrated the contact algorithm in the

* Corresponding author: Thaileng Oeng
E-mail: oeng.thaileng@itc.edu.kh; Tel: +855-86-311-323

model to solve the non interpenetration between the layers. On the other hand, more recently, [11] verified the effectiveness of uplift-restricted and slip-permitted connectors in alleviating crack formation in the negative-moment region of steel-concrete composite beams and improve the engineering adaptability of connectors, this paper proposes a modified uplift-restricted and slip-permitted connector. Static load tests and theoretical analysis were conducted on two overhanging beams with connectors and ordinary studs to analyze the influence of different stud forms on the deflection, crack, and slip in the negative-moment region. For the study of the nonlinear behavior of composite members, full composite models based on displacement interpolation functions with fiber discretization of the cross section and uniaxial stress-strain relations of the constituent materials, as proposed by [12] for the analysis of composite columns under uniaxial bending and [13] under biaxial bending. For the connector, Shear stud connectors are widely used in steel-concrete composite structures to resist shear and tensile loads at the steel-concrete interface. In the literature, extensive researches [14-18] have been conducted to study the behavior of connectors under static and/or fatigue loading. Most of the research works are focused on the shear response of the stud connector. The stud connectors under combined tension and shear have received more attention in the last decades due to the increase of using composite constructions. In this point of view, the behavior of stud connector under shear loading, tension loading and combination of both are presented.

This research paper presents an in-depth numerical modeling for planar two-layer composite beam with partial interaction, taking into account longitudinal slip and vertical uplift. For accounting those factors, the connectors are modeled by the two-directional springs. The horizontal one is parallel to the contact surface at the interface of the two layers, while the vertical one is orthogonal to the contact surface. The horizontal and the vertical springs are used to capture slip and uplift effects in the composite beam, respectively. In practical term, the penetration between layers (negative uplift) is not permitted. This requirement is presented by contact conditions which is solved by using contact resolution algorithm. This work focuses on material and geometrically nonlinear analysis (co-rotational approach): FE formulation will be conducted using displacement-based. Moreover, the connection model accounts for the interaction between the shear and tension force of the connector is proposed and used in the FE model.

The paper is structured as follows: **Section 2** outlines the methodology, encompassing the analysis of nonlinear geometry and material behavior, including the behavior of the connector. **Section 3** presents the results and discussion, providing insights to evaluate the proposed formulation and support the conclusions drawn in **Section 4**.

2. METHODOLOGY

The composite beam element with continuous bonding comprises numerous unconnected beam elements and connector elements. According to [19], their research introduced field equations describing the mechanical behavior of a shear deformable two-layer composite beam with partial shear interaction under large displacements, which are solved using the corotational frame method. This approach is primarily based on the kinematic assumption that displacements and rotations may be arbitrarily large, while deformation remains small. To account for the nonlinear behavior of materials, a displacement-based formulation is presented.

2.1 Local linear element

- *Displacement field*

The displacement field of a planar composite beam consists of two axial translations u_a and u_b in x-direction, two vertical translations v_a and v_b in y-direction and two rotations θ_a and θ_b around z-axis. The degree of freedom of the planar composite beam element without rigid body mode is:

$$\mathbf{q} = [u_b^i, v_b^i, \theta_b^i, u_a^i, v_a^i, \theta_a^i, u_b^j, v_b^j, \theta_b^j, u_a^j, v_a^j, \theta_a^j] \quad (\text{Eq. 1})$$

where the subscriptions a and b represents steel and concrete layer, respectively ($i = a, b$).

- *Interlayer slip and gap*

Slip is the difference of horizontal displacement between the concrete layer and steel layer at the interface. Because of the deformed cross-section, the terms of rotations of both layers are added into the expression of slip as following:

$$s = u_b - u_a + (h_a \theta_a + h_b \theta_b) \quad (\text{Eq. 2})$$

in which h_a and h_b are the distance between the centroid of both layers a and b, respectfully.

Gap is the difference of vertical displacement between the concrete layer and steel layer at the interface:

$$g = v_b - v_a \quad (\text{Eq. 3})$$

The combination of an unconnected composite beam element and two connector elements results in a connected composite beam element. The stiffness matrix was presented in [20].

2.2 Corotational framework

As mentioned earlier, the co-rotational method is adopted to take into account the geometric non linearity. This approach is a priory based on the kinematic assumptions that

the displacements and the rotations may be arbitrarily large, but the deformation is small. The advantage of using the co-rotational approach is that the geometrically linear finite element formulation can be reused and automatically transformed into a geometrically nonlinear formulation.

- *Beam kinematics*

The co-rotational description of the kinematic of a deformable body assumes that the motion of a beam element can be decomposed into a motion relative to a rigid frame, that follows the element as it deforms, and the rigid body motion of the frame. In finite element implementations, this decomposition is performed by defining a local reference attached to the element.

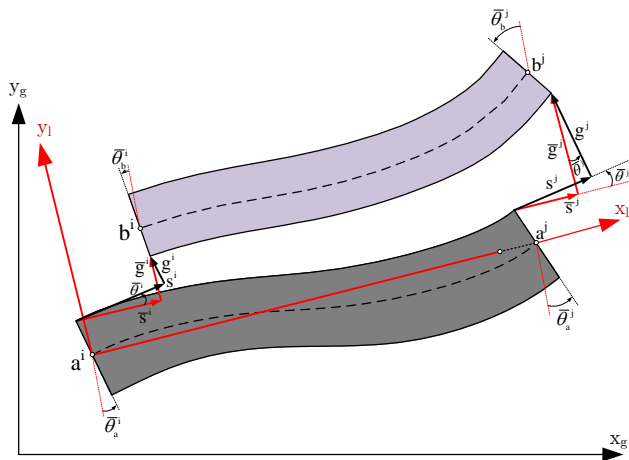


Fig.1. Co-rotational kinematics: slip and gap

The origin of the co-rotational frame is taken at the node a^i which corresponds to the centroid of the lower layer cross-section, see Fig.1. The rigid rotation of the x_1 axis, α , is obtained by using the geometrical relation in Fig.2.

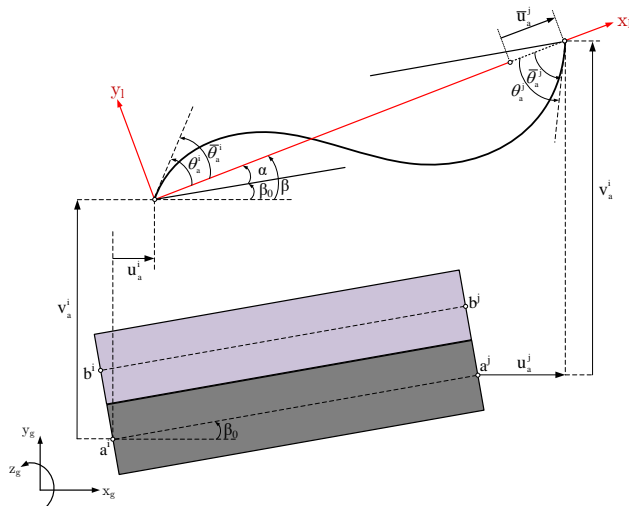


Fig.2. Initial and deformed configuration

- *Element formulation*

Once the relationship between local and global variables is established, the rigid body motions can be removed from the element displacement field. This can be achieved by calculating the local displacements and it was described in [20].

- *Equilibrium equation*

Consider a composite beam element subjected to external forces consisting of a distributed load p_y on the upper layer in the y -direction and nodal external forces \mathbf{Q}_l at the two end nodes of the element, see Fig.3.

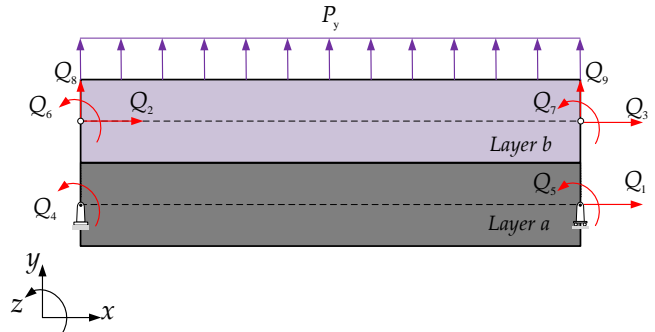


Fig.3. Nodal forces in composite beam element without rigid body mode

Let $\delta \mathbf{q}_l$ be a vector collecting all virtual displacements of the end nodes. The virtual work principle for the composite beam element can be written as:

$$\delta \Pi = \int_{\Omega_a} \delta \varepsilon_a \sigma_a d\Omega_a - \int_{\Omega_b} \delta \varepsilon_b \sigma_b d\Omega_b + \int_L [\delta \bar{s} D_{sc} + \delta \bar{g} V_{sc}] dx - \int_L \delta \bar{v}_b p_y dx - \delta \mathbf{q}_l^T \mathbf{Q}_l = 0 \quad (\text{Eq. 4})$$

where σ_a and σ_b are the axial stress on the lower (Ω_a) and upper area (Ω_b), respectively. D_{sc} and V_{sc} are the shear and vertical uplift force, respectively, in the connection.

2.3 Displacement-based formulation

The displacement-based (DB) formulation is a method used in structural analysis, particularly in finite element analysis (FEA). It is derived from the equilibrium equation by considering the displacement fields as the primary unknowns. It should be noted that the displacement fields are approximated between the element nodal degrees of freedom using shape functions. The displacement fields \mathbf{d} can be expressed as a function of nodal displacement \mathbf{q} as:

$$\mathbf{d}(x) = \mathbf{a}(x)\mathbf{q} \quad (\text{Eq. 5})$$

Where $\mathbf{a}(x) = [\mathbf{a}_{v_b}(x), \mathbf{a}_{v_a}(x), \mathbf{a}_{\theta_b}(x), \mathbf{a}_{\theta_a}(x)]^T$ is the shape function matrix and \mathbf{q} is expressed in Fig.4. and as follows:

$$\mathbf{q}(x) = [\bar{u}_b^i \ \bar{v}_b^i \ \bar{\theta}_b^i \ \bar{u}_a^i \ \bar{v}_a^i \ \bar{\theta}_a^i \ \bar{u}_b^m \ \bar{v}_b^m \ \bar{\theta}_b^m \ \bar{u}_a^m \ \bar{v}_a^m \ \bar{\theta}_a^m \ \bar{u}_b^j \ \bar{v}_b^j \ \bar{\theta}_b^j \ \bar{u}_a^j \ \bar{v}_a^j \ \bar{\theta}_a^j \ \bar{u}_b^{m1} \ \bar{u}_b^{m2} \ \bar{u}_b^{m3} \ \bar{v}_b^m \ \bar{\theta}_b^m \ \bar{u}_a^{m1} \ \bar{u}_a^{m2} \ \bar{u}_a^{m3} \ \bar{v}_a^m \ \bar{\theta}_a^m]^T$$

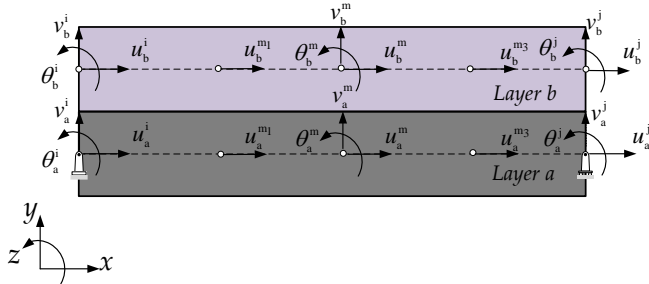


Fig.4. Displacement degrees of freedom

The sectional deformation vector $\mathbf{e}(x)$ in $\tilde{\mathbf{c}}\mathbf{d} - \mathbf{e} = \mathbf{0}$ is related to the nodal displacements by:

$$\mathbf{d}(x) = \mathbf{B}(x)\mathbf{q} \tag{Eq. 6}$$

in which $\mathbf{B}(x) = \tilde{\mathbf{c}}\mathbf{a}(x)$, \mathbf{e} is the vector collecting the generalised strains, given by: $\mathbf{d} = [\varepsilon_a, \kappa_a, \varepsilon_b, \kappa_b, \bar{s}, \bar{g}]^T$ and

$$\tilde{\mathbf{c}} = \begin{bmatrix} \frac{d}{dx} & 0 & 0 & 0 \\ 0 & \frac{d^2}{dx^2} & 0 & 0 \\ 0 & 0 & \frac{d}{dx} & 0 \\ 0 & 0 & 0 & \frac{d^2}{dx^2} \\ -1 & h_a \frac{d}{dx} & 1 & h_b \frac{d}{dx} \\ 0 & -1 & 0 & 1 \end{bmatrix}$$

2.4 Non-penetration condition

The two layers of the composite beam element, initially in contact over the element length, may partially separate (vertical uplift) or bear (contact) from one to another under a particular loading condition. To solve the contact problem, several resolution methods are available, see among others [21-22]. The non-penetration condition between the layers imposes that:

$$\bar{g}(x) = \bar{v}_b(x) - \bar{v}_a(x) = \mathbf{a}_g(x)\mathbf{q} \geq 0 \tag{Eq. 7}$$

where $\mathbf{a}_g(x) = \mathbf{a}_{v_b}(x) - \mathbf{a}_{v_a}(x)$. To take into account the non-penetration condition, the augmented Lagrangian term is added to the virtualwork principal as:

$$\delta \bar{\Pi}(\mathbf{q}) = \delta \Pi(\mathbf{q}) + \delta \mathbf{q}^T [\bar{\lambda} \mathbf{a}_g^T(x) + p \mathbf{a}_g^T(x) \mathbf{a}_g(x) \mathbf{q}] = 0 \tag{Eq. 8}$$

where $\bar{\lambda}$ is the so-called Lagrangian multiplier and p is a penalty parameter. Newton–Raphson method may be used to solve the nonlinear equation (Eq. 8) for a fixed known Lagrange multiplier $\bar{\lambda}$ by following the so-called Uzawa updating scheme.

2.5 Behavior of connector

Shear stud connectors are widely used in steel-concrete composite structures to resist shear and tensile loads at the steel-concrete interface. In the literature, extensive researches [14-17] have been conducted to study the behavior of connectors under static and/or fatigue loading.

- Shear behavior of connector

The shear behavior of connectors, such as headed studs or welded shear connectors, depends on the cross-sectional area of the stud shank and the ultimate strength of the stud material. Some existing shear strength formulations for a shear stud connector are evaluated herein [15,23,24]

$$D_{u,Kim} = 0.725 A_{sc} f_u \tag{Eq. 9}$$

$$D_{u,EU4} = \min(0.29 \alpha d^2 \sqrt{E_{cm} f_c}, 0.8 \pi d^2 f_u / 4) \tag{Eq. 10}$$

$$D_{u,AASHTO} = 0.5 A_{sc} \sqrt{E_{cm} f_c} \leq A_{sc} f_u \tag{Eq. 11}$$

where: d the stud shank diameter [mm], A_{sc} is the cross area of the stud shank [mm²], f_c is the concrete compressive strength [MPa], E_{cm} is the Young’s modulus of concrete [MPa], f_u is the ultimate strength of the stud material [MPa].

- Tensile behavior of connector

The pull-out strength, also known as the tensile strength, of a stud connector represents the maximum amount of force that can be applied to the connector before it fails. It measures the connector’s resistance to pull away from the anchored material. It is determined by various factors, including the material, properties and dimensions of the connector, and the method of installation [25]. The pull-out failure of a shear stud connector is avoid if $d_h < 1.71d$:

$$V_{u,kips} = \Psi_{c,p} 8 A_{brg, inches^2} f_{c,ksi} \tag{Eq. 12}$$

where: $A_{brg, inches^2} = \frac{\pi}{4} (d_{h, inches}^2 - d_{i, inches}^2)$

$\Psi_{c,p} = 1.4$. The unit of forces, length and strength are in kip, inches and ksi, respectively.

- *Coupled connector model*

Takami et Al, 1999 [18], proposed an circular interaction relation under the form of Eq. 13 as below:

$$\left(\frac{D_{sc}}{D_u}\right)^2 + \left(\frac{V_{sc}}{V_u}\right)^2 \leq 1 \quad \text{(Eq. 13)}$$

The model of the coupled stud connector shown in Fig. 5 is then utilized in our presented finite element model with the return mapping algorithm, which includes a yield criterion that accounts for the interaction between the shear and tensile behavior of the connector.

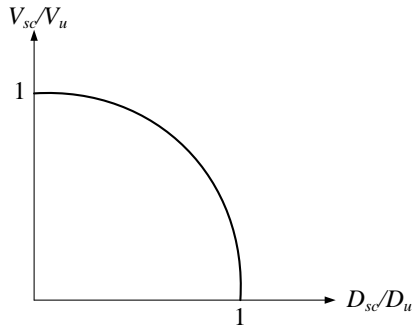


Fig.5. Interacted forces in stud connector proposed by [18].

3. RESULTS

The developed finite element models, incorporating the nonlinear behavior of concrete, steel, and connectors, will be assessed by comparing their results with experimental tests and analyzing the adoption of the DB method. Additionally, the influence of coupled/uncoupled connector model is illustrated.

3.1 Simply supported composite beam PI4 (Validation)

The composite beam PI4, which was studied by [26] has 5m length with a simply supported condition.

This composite beam is constructed by 800 mm×100 mm concrete slab and IPE400 steel beam with the geometrical details in Fig.6. The parametric study, the behavior of materials are following the utilization in [26]. The analysis of beam PI4 is performed using the displacement-based with various number of elements and it is presented in this chapter and implemented into co-rotational framework Section 2.2.

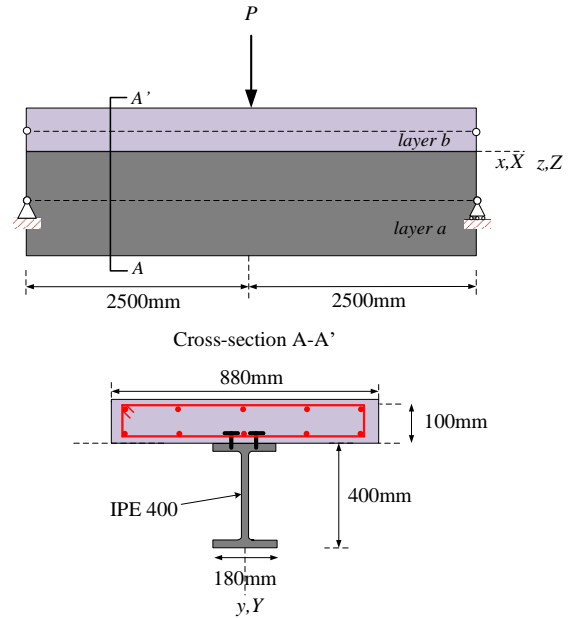


Fig.6. Simply supported composite beam PI4 [26]

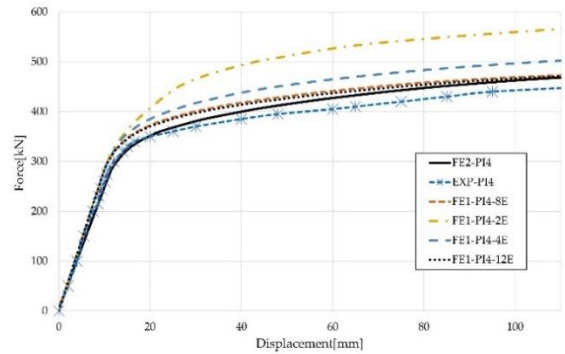


Fig.7. Comparison of load-vertical displacement

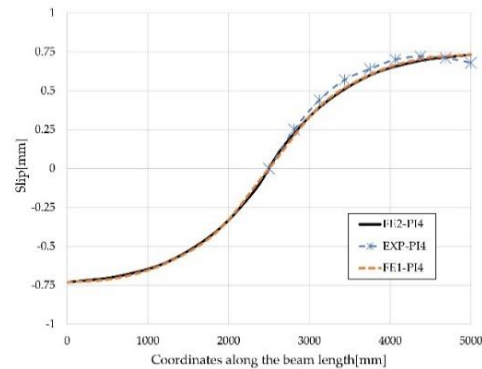


Fig.8. Slip distribution of beam PI4 at P=297 kN

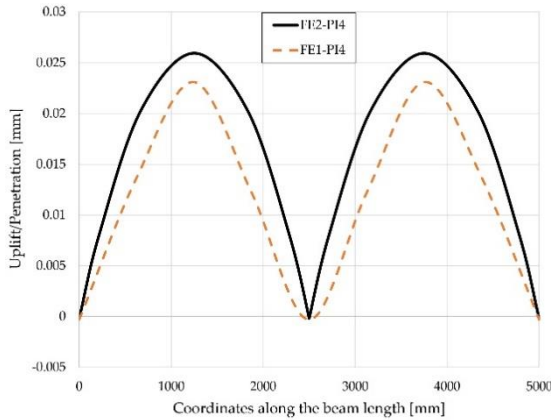


Fig.9. Uplift distribution of beam PI4 at P=297 kN

Fig.7 presents the relationship of applied force-vertical displacements at mid-span of composite beam with different computations as follows:

- EXP-PI4: results by experimental data of Abdel Aziz [26].
- FE1-PI4-2E, FE1-PI4-4E, FE1-PI4-8E, FE1-PI4-12E: results by displacement-based formulation using 2, 4, 8, 12 elements, respectively.
- FE2-PI4: results by mixed formulation by [20]

It can be seen that all formulations give essentially the same force-displacement curve in elastic range. Exceed that, we observe that more elements are required when the displacement-based formulation is used. In the results shown by Fig.7, it requires 8 or 12 elements for displacement-based formulation to get a satisfactory result. Furthermore, the slip and uplift distribution is also validated with existing model results, as shown in Fig.8 and Fig.9. Fig.9 can be adjusted using a contact algorithm at the element level, where very small and negligible penetration was observed along the interface of the beam. It is reasonable to expect some uplift when treating non-penetration conditions.

3.2 Continuous composite beam CTB1

In this example, we will consider the two-span-continuous composite beam CTB1 (4m and 5m long) designed and tested by [27]. We denote the 4m and 5m span of the beam by short and long span, respectively. The beam is subjected to a single concentrated load P at the middle of the short span.

The cross-section of CTB1 consisted of an IPE200 steel beam and a concrete slab 800mm × 100mm as depicted in Fig. 10.

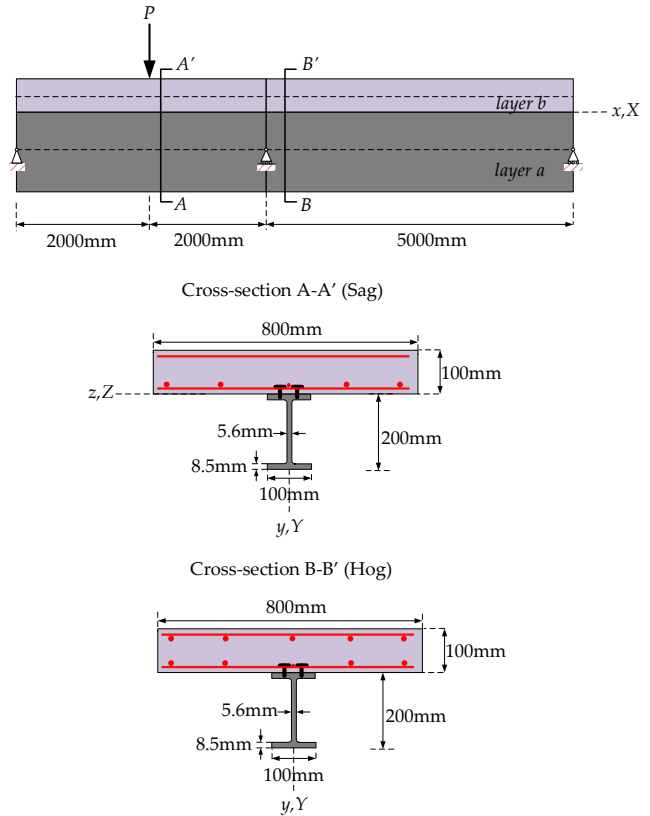


Fig.10. Continuous composite beam CTB1

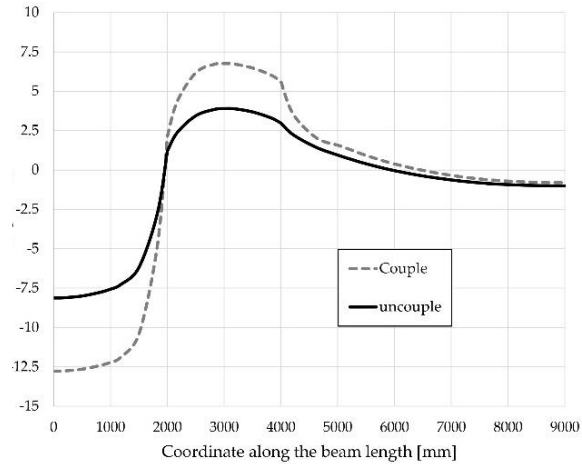


Fig.11. Slip distribution at P=143 kN

We observe that both models provide an ultimate load of 143 kN. At this load level, we observe a significant difference between the vertical displacements obtained with the coupled and uncoupled models. This can be explained by the distribution of slip and uplift at $P = 143$ kN depicted in Fig.11

and Fig.12. As expected, in Fig.11, the coupled connector model provided larger slip value than the uncoupled one. This is because the strength of the connector is reduced in the coupled model.

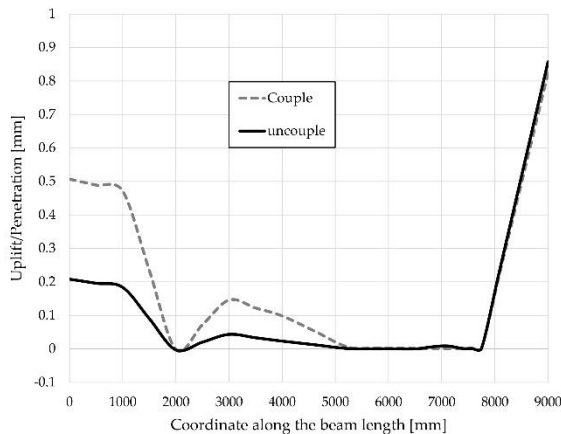


Fig.12. Slip distribution at $P=143$ kN

This is because the strength of the connector is reduced in the coupled model. Besides, as illustrated in Fig.12, the contact algorithm handled the non-penetrated condition very well, resulting in a maximum penetration of 0.0015mm which is very small and negligible. The results indicate that there is no difference in slip and uplift when the imposed load is within the elastic range. However, they become significantly different in plastic domain.

4. Conclusion

This research presents the development of displacement-based formulations for the nonlinear analysis of two-layer beams, taking into account the non-penetration condition. Node-to-node contact conditions are imposed by augmented Lagrangian conditions in these models. The computations employed displacement-based formulations with geometrical nonlinearity, yielding good agreement with both experimental results and existing models' results. However, the displacement-based formulation required a larger number of elements to obtain satisfactory results. Another significant aspect pertains to the replacement of the concrete layer. In the model of the connector, the coupled and uncoupled models exhibit a good agreement during the elastic deformation stage. However, beyond that stage, the connector behaves more stiff with the uncoupled connector model.

ACKNOWLEDGMENTS

In recognition of collaborative efforts, the authors extend their appreciation to the top standardized engineering institutions ITC (Cambodia) and TMU (Canada), alongside the financial backing provided by the SEED program

throughout the duration of the research conducted within the Canadian jurisdiction.

REFERENCES

- [1] Newmark, N. M. (1951). Test and analysis of composite beam with incomplete interaction. Proc. of the society for experimental stress analysis, 9(1), 75-92.
- [2] Faella, C., Martinelli, E., & Nigro, E. (2002). Steel and concrete composite beams with flexible shear connection: "exact" analytical expression of the stiffness matrix and applications. Computers & structures, 80(11), 1001-1009.
- [3] Girhammar, U. A., & Gopu, V. K. (1993). Composite beam-columns with interlayer slip—exact analysis. Journal of Structural Engineering, 119(4), 1265-1282.
- [4] Girhammar, U. A., & Pan, D. H. (2007). Exact static analysis of partially composite beams and beam-columns. International Journal of Mechanical Sciences, 49(2), 239-255.
- [5] Keo, P., Nguyen, Q. H., Somja, H., & Hjiat, M. (2016). Derivation of the exact stiffness matrix of shear-deformable multi-layered beam element in partial interaction. Finite Elements in Analysis and Design, 112, 40-49.
- [6] Nguyen, Q. H., Martinelli, E., & Hjiat, M. (2011). Derivation of the exact stiffness matrix for a two-layer Timoshenko beam element with partial interaction. Engineering Structures, 33(2), 298-307.
- [7] Ranzi, G., Bradford, M. A., & Uy, B. (2004). A direct stiffness analysis of a composite beam with partial interaction. International Journal for Numerical Methods in Engineering, 61(5), 657-672.
- [8] Adekola, A. O. (1968). Partial interaction between elastically connected elements of a composite beam. International Journal of Solids and Structures, 4(11), 1125-1135.
- [9] Jean-Marie A. and K. Abdel A. (1985). Ultimate state analysis of composite beam taking into account uplift effects at the steel-concrete interface. Revue Construction Métallique, 4:3-36.
- [10] Guezouli, S., & Alhasawi, A. (2014). A new concept for the contact at the interface of steel-concrete composite beams. Finite Elements in Analysis and Design, 87, 32-42.
- [11] Bu, J., Cao, W., Wang, X., & Zhang, L. (2023). Experimental Research on the Mechanical Properties of MURSP-Type Steel-Concrete Composite Beams in Negative-Moment Region. Buildings, 13(4), 1095.
- [12] Mirza, S. A., & Skrabek, B. W. (1991). Reliability of short composite beam-column strength interaction. Journal of Structural Engineering, 117(8), 2320-2339.

- [13] El-Tawil, S., Sanz-Picon, C. F., & Deierlein, G. G. (1995). Evaluation of ACI 318 and AISC (LRFD) strength provisions for composite beam-columns. *Journal of Constructional Steel Research*, 34(1), 103-123.
- [14] Ollgaard, J. G., Slutter, R. G., & Fisher, J. W. (1971). Shear strength of stud connectors in lightweight and normal weight concrete, *AISC Eng'g Jr.*, April 1971 (71-10). *AISC Engineering journal*, 55-34.
- [15] Oehlers, D. J., & Coughlan, C. G. (1986). The shear stiffness of stud shear connections in composite beams. *Journal of Constructional Steel Research*, 6(4), 273-284.
- [16] Okubo, N., Kurita, A., Komatsu, K., & Ishihara, Y. (2002). Experimental study on static and fatigue characteristics of grouped stud. *J. Structural Eng., JSCE*, 48, 1391-1397.
- [17] McMackin, P. J. (1973). Headed steel anchors under combined loading. *AISC Engineering Journal*, 43-52.
- Shim, C., Kim, J., Chang, S. P., & Chung, C. H. (2000). The behaviour of shear connections in a composite beam with a full-depth precast slab. *Proceedings of the Institution of Civil Engineers-Structures and Buildings*, 140(1), 101-110.
- [18] Takami, K., Nishi, K., & Hamada, S. (1999). Shear strength of headed stud shear connector subjected to tensile load. *Journal of Constructional Steel*, 7, 233-240.
- [19] Nguyen, Q. H. (2009). Modelling of the nonlinear behaviour of composite beams taking into account time effects (Doctoral dissertation, Dissertation, INSA de Rennes, France).
- [20] Oeng, T., Keo, P., Guezouli, S., & Hjjaj, M. (2023). Large displacement analysis of two-layer beam-columns taking into account slip and uplift. *Engineering Computations*, 40(1), 265-295.
- [21] Wriggers, P. (2006). *Computational contact mechanics* (Vol. 2, p. 25). T. A. Laursen (Ed.). Berlin: Springer.
- [22] Leonetti, L., Liguori, F. S., Magisano, D., Kiendl, J., Reali, A., & Garcea, G. (2020). A robust penalty coupling of non-matching isogeometric Kirchhoff–Love shell patches in large deformations. *Computer Methods in Applied Mechanics and Engineering*, 371, 113289.
- [23] EN1994-1-1 (2004) *Design of Composite Steel and Concrete Structures, Part 1.1, General rules and rules for building*.
- [24] Toorak AASHTO-LRFD Zokaie. (2000), “AASHTO-LRFD live load distribution specifications”. In: *Journal of bridge engineering* 5.2 pp. 131–138. Code,
- [25] A.C.I. (2005). *Building code requirements for structural concrete (ACI 318-05) and commentary (ACI 318R-05)*. American Concrete Institute, Farmington Hills, Mich.
- [26] Abdel Aziz, K. (1986). Numerical modeling and experimental study of composite beams with partial or spaced shear connection (Doctoral dissertation, INSA Rennes).
- [27] Ansourian, P. (1982). Experiments on continuous composite beams. *Proceedings of the Institution of Civil Engineers*, 73(1), 26-51.